PHYSICAL REVIEW D **80,** 126009 (2009)

Vortex and droplet engineering in a holographic superconductor

Tameem Albash* and Clifford V. Johnson†

[1]*Department of Physics and Astronomy, University of Southern California, Los Angeles, CA 90089-0484, USA*

(Received 23 August 2009; published 18 December 2009)

We give a detailed account of the construction of nontrivial localized solutions in a 2 + 1 dimensional model of superconductors using a 3 + 1 dimensional gravitational dual theory of a black hole coupled to a scalar field. The solutions are found in the presence of a background magnetic field. We use numerical and analytic techniques to solve the full Maxwell-scalar equations of motion in the background geometry, finding condensate droplet solutions, and vortex solutions possessing a conserved winding number. These solutions and their properties, which we uncover, help shed light on key features of the (B, T) phase diagram.

DOI: 10.1103/PhysRevD.80.126009 PACS numbers: 11.25.Tq, 04.65.+e, 11.15.Pg, 11.25.−w

I. INTRODUCTION

An holographic model of some of the key phenomenological attributes of superconductivity in 2 + 1 dimensions was proposed in Ref. [1]. It works roughly as follows (a more detailed review will follow in the next section). The dual is a simple model of gravity in four dimensions (with negative cosmological constant) coupled to a $U(1)$ gauge field and a minimally coupled charged complex scalar Ψ. Asymptotic values of the scalar on the boundary correspond to the vacuum expectation value (vev) of a charged operator in the 2 + 1 dimensional theory. For high temperatures (relative to a scale set by nonzero charge density in the model) the system is in a normal phase represented by a charged black hole solution in the gravitational dual with the scalar set to zero. At a critical temperature the system undergoes a phase transition, the $U(1)$ getting spontaneously broken by a nonzero vev of the charged operator.[1] The gravitational description of this is a charged black hole with a nontrivial scalar profile that gives the vev on the boundary. This means that the black hole has ''scalar hair'' in this regime. (For a discussion of violations of no-hair theorems in this context, see Ref. [3]. There, it was shown that it is possible in this context, for large enough charges, equivalent to the low temperature regime here.) The authors of Ref. [1] showed using linear response theory that the DC conductivity of this new phase diverges in a manner consistent with the expectation that the system is in a superconducting phase[2] The authors carried out further study of the system in Ref. [2].

Our focus in this paper is the system in an external magnetic field, continuing the work we began in Ref. [6]. Generically, for nonzero magnetic field B filling the two spatial dimensions, it is inconsistent to have nontrivial spatially independent solutions on the boundary, and we present and study two classes of localized solutions in some detail. The first is a ''droplet'' solution, the prototype of which was found in our earlier work [6] as a strip in 2D (straightforwardly generalized to circular symmetry in Ref. [2]), and the second is a vortex solution, with integer winding number $\xi \in \mathbb{Z}$, which is entirely new. We obtain these as full solutions of the Maxwellscalar sector in a limit, and determine a number of their properties.

Our analysis in various connected limits shows where these solutions can exist in the (B, T) plane. There is a critical line below which droplets are not found, while vortices can be found there. Our interpretation is that this region is the superconducting phase, and that for nonzero B, the vortices develop, trapping the magnetic flux into filaments, as is familiar in type II superconductors. Above the critical line, the system leaves the superconducting phase, and either forms droplets of condensate or simply reverts to the normal phase (dual to a dyonic black hole with zero scalar everywhere, which may well yield lower action than the droplets if we had backreacting solutions to work with).

In Sec. II we review the model, and discuss the two limits in which most of our studies will be carried out. Section III reviews the spatially independent solution corresponding to the prototype superconducting solution. We briefly discuss our numerical approach to finding the solution as a warm up for the more difficult problems in the sequel. Section IV presents our search for and construction of the nontrivial spatially dependent solutions corresponding to condensate droplets and to vortices. We discuss the numerical methods we used to find them, and then examine a number of their properties. Section V examines aspects of the solutions' stability. We conclude in Sec. V, and we also present two appendices. One appendix establishes the normalization of our gauge/gravity dual dictionary, while the other discusses the flux quantization in our vortices.

*talbash@usc.edu

†johnson1@usc.edu

[1]Strictly speaking, the $U(1)$ that is broken is global on the boundary, but it can be gauged in a number of ways without affecting the conclusions. See *e.g.* Ref. [2]. Note that a global $U(1)$ does not restrict us to a spatially independent magnetic field.

[2]Other holographic superconductors are available. See *e.g.* Refs. [4,5].

II. THE MODEL, AND TWO LIMITS

A. The model

The holographic model of superconductivity in $2+1$ dimensions proposed in Ref. [1] is a model of gravity in four dimensions coupled to a $U(1)$ gauge field and a minimally coupled charged complex scalar Ψ with potential $V(|\Psi|) = -2|\Psi|^2/L^2$. There is a negative cosmological constant that defines a scale L *via* $\Lambda = -3/L^2$. The action is:

$$S_{\rm bulk} = \frac{1}{2\kappa_4^2}\int d^4x\sqrt{-G}\Big\{R + \frac{6}{L^2} + L^2\Big(-\frac{1}{4}F^2 - |\partial\Psi - igA\Psi|^2 - V(|\Psi|)\Big)\Big\}, \tag{1}$$

where $\kappa_4^2 = 8\pi G_N$ is the gravitational coupling and our signature is $(-+++)$.

We will use coordinates (t, z, r, ϕ) for much of our discussion, with t time, (r, ϕ) forming a plane, and z a "radial" coordinate for our asymptotically AdS_4 spacetimes such that $z = 0$ is the boundary at infinity. The AdS_4 metric is:

$$ds^2 = \frac{L^2}{z^2}(dz^2 - dt^2 + dr^2 + r^2 d\phi^2). \tag{2}$$

Note that the mass of the scalar $m_\Psi^2 = -2/L^2$ is above the Breitenlohner-Freedman stability bound [7] $m_{\rm BF}^2 = -9/4L^2$ for scalars in AdS_4. We will write the scalar as:

$$\Psi = \frac{\tilde\rho}{\sqrt{2}L}\exp(i\theta). \tag{3}$$

Near the boundary $z = 0$ we have:

$$\tilde\rho \to \tilde\rho_1 z + \tilde\rho_2 z^2, \tag{4}$$

where $\tilde\rho_i$ $(i = 1, 2)$ sets the vacuum expectation value (vev) of an operator $\mathcal{O}_i$ with dimension $\Delta = i$ [8]. Only one of these vevs can be nonzero at a time, and we will choose to study the case of $i = 1$, for much of the paper. Our charged operator will be the order parameter for the spontaneous breaking of the $U(1)$ symmetry. A gauge field of the form $A = A_t dt$ does not give an electric field in the dual theory on (r, ϕ), but defines instead [9] a $U(1)$ charge density, ρ and its conjugate chemical potential μ, as we will recall below.

Black holes in this study will be planar, *i.e.,* their horizons are an (r, ϕ) plane at some finite $z = z_h$. In the familiar manner, their Hawking temperature T and mass per unit horizon area $\varepsilon = M/\mathcal{V}$, corresponds to the dual $2+1$ dimensional system at temperature T and with energy density ε. Generically, the black hole will couple to the gauge sector, having some profile for the field A_t. The temperature T will have dependence on the charge density parameter ρ. This is quite natural since without the charge density there is no other scale in the theory, and there would be no meaning to a high or low temperature phase, and hence no possibility of a phase transition.

The high T phase of the theory is simply the charged black hole [Reissner-Nordström (AdS-RN)] with the scalar Ψ vanishing. This corresponds to the nonsuperconducting or "normal" phase of the theory, where the order parameter vanishes. The mass of the scalar Ψ is set not just by $V(|\Psi|)$ but by the density ρ through the coupling to the gauge field. In fact m_Ψ^2 decreases with T until at T_c it goes below $m_{\rm BF}^2$, becoming tachyonic. The theory seeks a new solution, in which the black hole is no longer AdS-RN, but one that has a nontrivial profile for Ψ.

In studying the system in a magnetic field background, there are some generic expectations to consider. The magnetic field B (which fills the two dimensions of the superconducting theory), also contributes to m_Ψ^2, *via* its square, but contributes with *opposite sign* to the electric contribution of the background. It therefore lowers the temperature T_c at which m_Ψ^2 falls below $m_{\rm BF}^2$, triggering the phase transition. On these grounds alone one then (naively) expects a critical line in the (B, T) plane connecting $(0, T_c)$ to some $(B_c, 0)$, but it is important to determine exactly what physics lies on either side of the line. Our solutions and our study of their properties help in establishing some of this. The solutions can be found by solving equations of motion in certain limits and we remind the reader of them in the next two subsections.

B. The decoupling limit

After a field redefinition:

$$A_\mu \to \frac{1}{g}A_\mu, \qquad \Psi \to \frac{1}{g}\Psi, \tag{5}$$

our action (1) becomes:

$$S_{\rm bulk} = \frac{1}{2\kappa_4^2}\int d^4x\sqrt{-G}\Big\{R + \frac{6}{L^2} + \frac{L^2}{g^2}\Big(-\frac{1}{4}F^2 - |\partial\Psi - iA\Psi|^2 + \frac{2}{L^2}\bar\Psi\Psi\Big)\Big\}. \tag{6}$$

If we consider the limit $g \to \infty$, then the Maxwell-scalar sector decouples from gravity. This allows us to work with a fixed uncharged background, which we take to be the AdS_4-Schwarzschild (AdS-Sch) black hole, given by:

$$ds^2 = \frac{L^2\alpha^2}{z^2}(-f(z)dt^2 + dr^2 + r^2 d\phi^2) + \frac{L^2}{z^2}\frac{1}{f(z)}dz^2, \tag{7}$$

where $f(z) = 1 - z^3$. The coordinate z is a dimensionless parameter scaled such that the event horizon is at $z_h = 1$. The Hawking temperature is given by the usual Gibbons-Hawking calculus [10]:

$$T = \frac{3}{4\pi}\alpha. \tag{8}$$

Note that α is related to the mass of the black hole:

$$\varepsilon = \frac{M}{\mathcal{V}} = \frac{L^2\alpha^3}{\kappa_4^2}, \tag{9}$$

where $\mathcal{V}$ is the volume of the (r, ϕ) plane. In terms of the two real fields $(\tilde{\rho}, \theta)$ into which we decomposed Ψ into in Eq. (3) we have:

$$\begin{aligned} -L^2|\partial\Psi - iA\Psi|^2 + 2\bar{\Psi}\Psi \\ = -\frac{1}{2}G^{\mu\nu}[\partial_\mu\tilde{\rho}\partial_\nu\tilde{\rho} + \tilde{\rho}^2(\partial_\mu\theta\partial_\nu\theta - 2A_\mu\partial_\nu\theta \\ + A_\mu A_\nu)] + \frac{1}{L^2}\tilde{\rho}^2. \end{aligned} \tag{10}$$

From the action, we derive the equation of motion for the fields $\tilde{\rho}$, θ, and A_μ:

$$\begin{aligned} \frac{1}{\sqrt{-G}}\partial_\mu(\sqrt{-G}G^{\mu\nu}\partial_\nu\tilde{\rho}) \\ -G^{\mu\nu}\tilde{\rho}(A_\mu - \partial_\mu\theta)(A_\nu - \partial_\nu\theta) + \frac{2}{L^2}\tilde{\rho} = 0, \\ -\frac{1}{\sqrt{-G}}\partial_\mu(\sqrt{-G}G^{\mu\nu}\tilde{\rho}^2(A_\nu - \partial_\nu\theta)) = 0, \\ \frac{1}{\sqrt{-G}}\partial_\nu(\sqrt{-G}G^{\nu\lambda}G^{\mu\sigma}F_{\lambda\sigma}) - \frac{G^{\mu\nu}}{L^2}\tilde{\rho}^2(A_\nu - \partial_\nu\theta) = 0. \end{aligned} \tag{11}$$

While the background itself will have no charge in this limit, there will of course still be a nontrivial gauge field A, and for an electric background $A = A_t dt$, we will have, as $z \to 0$:

$$\frac{A_t}{\alpha} \equiv \tilde{A}_t \to \mu - \rho z, \tag{12}$$

defining a chemical potential μ and a charge density ρ.

C. The probe limit

Sometimes we will also work in a probe limit, where we take the scalar in the Maxwell-scalar sector to be small, and hence not back–reacting on either the geometry. In general, we can do this at arbitrary g. (We will combine this with the decoupling limit ($g \to \infty$) for one case, as we shall see later in Sec. IV A 2.) For finite g we will consider our small nonbackreacting scalar to be moving in a dyonic Reissner-Nordström background, given by [11]:

$$\begin{aligned} ds^2 &= \frac{L^2\alpha^2}{z^2}(-f(z)dt^2 + dr^2 + r^2d\phi^2) + \frac{L^2}{z^2}\frac{dz^2}{f(z)}, \\ F &= 2h\alpha^2 r dr \wedge d\phi + 2q\alpha dz \wedge dt, \\ f(z) &= 1 + (h^2+q^2)z^4 - (1 + h^2 + q^2)z^3 \\ &= (1-z)(z^2 + z + 1 - (h^2+q^2)z^3). \end{aligned} \tag{13}$$

The temperature and charge density are given by:

$$\begin{aligned} T = \frac{1}{\beta} = \frac{\alpha}{4\pi}(3 - h^2 - q^2), \\ \rho = \frac{1}{\mathcal{V}\beta}\frac{\delta S_{\text{on-shell}}}{\delta A_t(z=0)} = -\frac{L^2}{\kappa_4^2}q\alpha^2. \end{aligned} \tag{14}$$

We choose a gauge such that the gauge field is written as:

$$A = h\alpha^2 r^2 d\phi + 2q\alpha(z-1)dt. \tag{15}$$

III. SPATIALLY INDEPENDENT SOLUTION

We begin by considering a spatially independent solution, reviewing the original presentation of Ref. [1], working in the decoupling limit of Sec. II B. We take an ansatz for the fields given by:

$$\theta \equiv \text{const}, \qquad \tilde{\rho} = \tilde{\rho}(z), \qquad A_t \equiv \alpha\tilde{A}_t(z), \qquad A_\phi = 0. \tag{16}$$

where $\tilde{\rho}$ and $\tilde{A}_t$ are dimensionless fields. The equations of motion are given by:

$$\begin{aligned} \partial_z^2\tilde{\rho} + \left(\frac{f'}{f} - \frac{2}{z}\right)\partial_z\tilde{\rho} + \frac{1}{f^2}\tilde{\rho}\tilde{A}_t^2 + \frac{2}{z^2 f}\tilde{\rho} = 0, \\ \partial_z^2\tilde{A}_t - \frac{1}{z^2 f}\tilde{\rho}^2\tilde{A}_t = 0. \end{aligned} \tag{17}$$

We can study the equations' behavior near the event horizon (*i.e.* as $z \to 1$):

$$\begin{aligned} \left[\partial_z\tilde{\rho} - \frac{2}{3}\tilde{\rho}\right]_{z=1} = 0, \\ \left[\partial_z^2\tilde{\rho} - \frac{5}{6}\partial_z\tilde{\rho} + \tilde{\rho} + \frac{1}{18}\tilde{\rho}(\partial_z\tilde{A}_t)^2\right]_{z=1} = 0, \\ \tilde{A}_t|_{z=1} = 0, \qquad \left[\partial_z^2\tilde{A}_t + \frac{1}{3}\tilde{\rho}^2\partial_z\tilde{A}_t\right]_{z=1} = 0. \end{aligned}$$

We note that the only free variables (to be chosen) at the event horizon are $\tilde{\rho}(1)$ (or $\partial_z\tilde{\rho}(1)$) and $\partial_z\tilde{A}_t(1)$. The other limit to study is to consider the behavior near the AdS boundary ($z \to 0$):

$$\begin{aligned} \left[\partial_z^2\tilde{\rho} - \frac{2}{z}\partial_z\tilde{\rho} + \frac{2}{z^2}\tilde{\rho}\right]_{z=0} = 0, \\ \left[\partial_z^2\tilde{A}_t - \frac{1}{z^2}\tilde{\rho}^2\tilde{A}_t\right]_{z=0} = 0, \end{aligned}$$

which has as solutions

$$\tilde{\rho}(z \to 0) \to \tilde{\rho}_1 z + \tilde{\rho}_2 z^2, \qquad \tilde{A}_t(z \to 0) \to \mu - \rho z, \tag{18}$$

where $\tilde{\rho}_1$, $\tilde{\rho}_2$, μ, and ρ are constants related to the vev of a $\Delta = 1$ operator, the vev of a $\Delta = 2$ operator, the chemical potential, and the charge density of the dual field theory, respectively. The solution for $\tilde{\rho}$ at the AdS boundary admits two normalizable modes, and therefore the constants are associated with vevs of two separate operators.

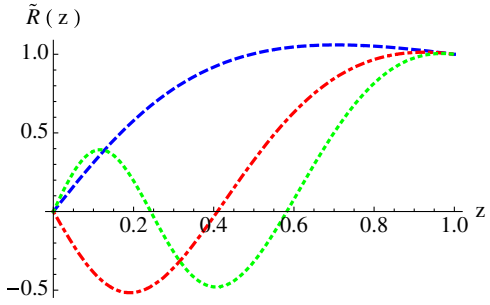

FIG. 1 (color online). Three solutions with the same $\tilde{R}(1)$ but different $\partial_z\tilde{A}_t(1)$ that satisfy Dirichlet boundary conditions at $z = 0$. The solutions are distinguished by the number of nodes (times they cross the z-axis) they have.

Only one of these vevs is to be nonzero at a time, and the two different gauge theories are related to each other *via* a Legendre transformation [8].

Numerical analysis

To simplify the numerical analysis, it is convenient to define a new field $\tilde{R}(z)$ such that:

$$\tilde{R}(z) = z\tilde{\rho}(z). \tag{19}$$

With this redefinition, the boundary condition of having either $\tilde{\rho}_1$ or $\tilde{\rho}_2$ in Eq. (18) to be zero becomes the requirement of having either a Dirichlet or a Neumann boundary condition on $\tilde{R}$ at the AdS boundary. The equations in the bulk of AdS are given by:

$$\partial_z^2\tilde{R} + \frac{f'}{f}\partial_z\tilde{R} + \frac{1}{f^2}\tilde{R}\tilde{A}_t^2 + \left(\frac{f'}{zf} - \frac{2}{z^2} + \frac{2}{z^2 f}\right)\tilde{R} = 0,$$
$$\partial_z^2\tilde{A}_t - \frac{1}{f}\tilde{R}^2\tilde{A}_t = 0, \tag{20}$$

and we solve them using a shooting method (discretizing using finite differences) with shooting conditions:

$$\tilde{R}(1) = \text{const}, \qquad \partial_z\tilde{R}(1) = -\frac{1}{3}\tilde{R}(1),$$
$$\partial_z^2\tilde{R}(1) = -\frac{5}{18}\tilde{R}(1) - \frac{1}{18}(\partial_z\tilde{A}_t(1))^2\tilde{R}(1). \qquad \tilde{A}_t(1) = 0,$$
$$\partial_z\tilde{A}_t(1) = \text{const}, \qquad \partial_z^2\tilde{A}_t(1) = -\frac{1}{3}\tilde{R}(1)^2\partial_z\tilde{A}_t(1). \tag{21}$$

The solution at $z = 0$ goes as:

$$\tilde{R}(z \to 0) = \tilde{R}_1 + \tilde{R}_2 z, \qquad \tilde{A}_t(z \to 0) = \mu - \rho z. \tag{22}$$

We fix $\tilde{R}(1)$ and then tune $\partial_z\tilde{A}_t(1)$ until the solution satisfies the necessary Dirichlet or Neumann boundary condition at $z = 0$. We then read off the scalar and also the value of ρ for that solution, which defines the temperature. We can determine T_c since there is a minimum charge density (over temperature squared) needed for the scalar field to condense. Note that there are multiple choices for $\partial_z\tilde{A}_t(1)$ that give the necessary boundary condition at the AdS boundary, sample solutions of which we present in Fig. 1. Solutions with a greater number of nodes are associated with higher chemical potential/charge density. These solutions are of a higher energy and so are thermodynamically unfavorable, therefore we only present results of the zero-node solutions in what follows. In Fig. 2 we show the solutions for the scalar values $\tilde{\rho}_{1,2}$ at the boundary which give the vevs of the operators $\mathcal{O}_{1,2}$. As anticipated, in each case, the vev of the operator is zero above $T/T_c = 1$. Below $T/T_c = 1$, it is not zero, showing the spontaneous breaking of the $U(1)$ symmetry.

IV. SPATIALLY DEPENDENT SOLUTIONS

A nonzero magnetic field B in the (r, ϕ) plane will correspond to some nonzero $A_\phi(r)$. In such a case, consistency of the solution requires the fields to have some spatial dependence in the plane. This situation was studied in the linear case in Ref. [6], (see also Ref. [2]) but here we consider the full nonlinear problem of Eq. (11). First, notice that the $U(1)$ gauge transformation acts as:

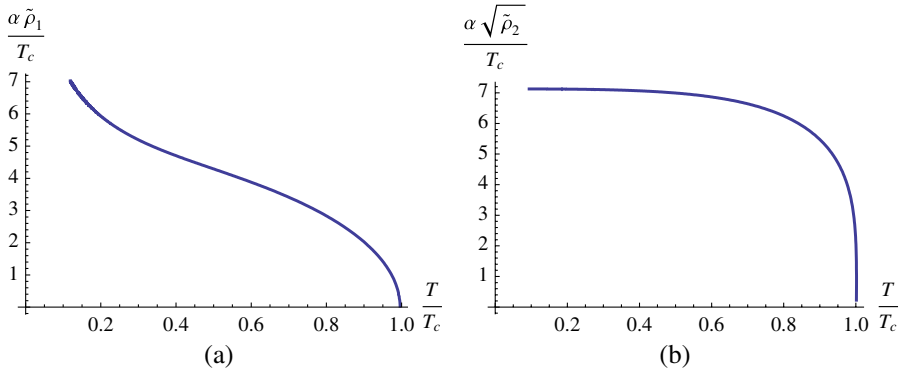

FIG. 2 (color online). Vacuum expectation values for the scalar. Here T_c is defined to be $0.226\alpha\sqrt{\rho}$ and $0.118\alpha\sqrt{\rho}$ for the $\Delta = 1$ and $\Delta = 2$ operator, respectively.

$$\rho \to \rho, \qquad \theta \to \theta + \Lambda, \qquad A_\mu \to A_\mu + \partial_\mu \Lambda. \quad (23)$$

In the previous section we chose θ to have no nontrivial dependence. Naively, it would seem that we can freely shift θ by gauge transformations. However, this freedom is only available if the gauge symmetry is not broken. We will return to this once we have constructed the solutions. This motivates us to consider the following ansatz:

$$\begin{aligned} \theta &\equiv \zeta + \xi\phi, \qquad \tilde{\rho} = \tilde{\rho}(\tilde{r}, z), \\ A_t &= \alpha \tilde{A}_t(\tilde{r}, z), \qquad A_\phi = \tilde{A}_\phi(\tilde{r}, z), \end{aligned} \quad (24)$$

where we have defined a dimensionless radial coordinate $\tilde{r} = \alpha r$, dimensionless fields $\tilde{\rho}$, $\tilde{A}_t$, and $\tilde{A}_\phi$, and (ζ, ξ) are constants where ξ is an integer. Under this ansatz, the equations of motion reduce to:

$$\begin{aligned} &\partial_z^2\tilde{\rho} + \left(\frac{f'}{f} - \frac{2}{z}\right)\partial_z\tilde{\rho} + \frac{1}{f}\left(\partial_{\tilde{r}}^2\tilde{\rho} + \frac{1}{\tilde{r}}\partial_{\tilde{r}}\tilde{\rho} - \frac{1}{\tilde{r}^2}\tilde{\rho}(\tilde{A}_\phi - \xi)^2\right) + \frac{1}{f^2}\tilde{\rho}\tilde{A}_t^2 + \frac{2}{z^2 f}\tilde{\rho} = 0, \\ &\partial_z^2\tilde{A}_\phi + \frac{f'}{f}\partial_z\tilde{A}_\phi + \frac{1}{f}\left(\partial_{\tilde{r}}^2\tilde{A}_\phi - \frac{1}{\tilde{r}}\partial_{\tilde{r}}\tilde{A}_\phi\right) - \frac{1}{z^2 f}\tilde{\rho}^2(\tilde{A}_\phi - \xi) = 0, \qquad \partial_z^2\tilde{A}_t + \frac{1}{f}\left(\partial_{\tilde{r}}^2\tilde{A}_t + \frac{1}{\tilde{r}}\partial_{\tilde{r}}\tilde{A}_t\right) - \frac{1}{z^2 f}\tilde{\rho}^2\tilde{A}_t = 0, \end{aligned} \quad (25)$$

where the equation of motion for the field θ is trivially satisfied by our ansatz. Near the event horizon, these equations reduce to the following conditions that must be satisfied:

$$\begin{aligned} &\left[\partial_{\tilde{r}}^2\tilde{\rho} + \frac{1}{\tilde{r}}\partial_{\tilde{r}}\tilde{\rho} - \frac{1}{\tilde{r}^2}\tilde{\rho}(\tilde{A}_\phi - \xi)^2 + 2\tilde{\rho} = 3\partial_z\tilde{\rho}\right]_{z=1}, \qquad \left[\partial_z^2\tilde{\rho} = -\frac{4}{3}\tilde{\rho} - \frac{1}{9}\tilde{\rho}(\partial_z\tilde{A}_t)^2\right]_{z=1}, \\ &\left[\partial_{\tilde{r}}^2\tilde{A}_\phi - \frac{1}{\tilde{r}}\partial_{\tilde{r}}\tilde{A}_\phi - (\tilde{A}_\phi - \xi)\tilde{\rho}^2 = 3\partial_z\tilde{A}_\phi\right]_{z=1}, \qquad \left[\partial_z^2\tilde{A}_\phi = \frac{2}{3}(\tilde{A}_\phi - \xi)\tilde{\rho}^2 - 2\partial_z\tilde{A}_\phi\right]_{z=1}, \\ &\tilde{A}_t(\tilde{r}, z = 1) = 0, \qquad \left[3\partial_z^2\tilde{A}_t = \partial_z\left(\partial_{\tilde{r}}^2\tilde{A}_t + \frac{1}{\tilde{r}}\partial_{\tilde{r}}\tilde{A}_t - \tilde{\rho}^2\tilde{A}_t\right) + 2\tilde{A}_t\tilde{\rho}^2\right]_{z=1}, \end{aligned} \quad (26)$$

where in the first equation we have used that $\tilde{A}_t(\tilde{r}, z = 1) = 0$. We now have three free functions to fix in these equations, $\partial_z\tilde{\rho}(\tilde{r}, z = 1)$, $\partial_z\tilde{A}_\phi(\tilde{r}, z = 1)$ and $\partial_z\tilde{A}_t(\tilde{r}, z = 1)$, which determine the spatial profile of the solutions at the event horizon. Note that in order to avoid a divergence in the equation for $\tilde{\rho}$ at $\tilde{r} = 0$, we must have that near $\tilde{r} = 0$, the field $\tilde{\rho}$ must go as $\tilde{r}^\xi$. This motivates the following field redefinitions:

$$\tilde{\rho} = z\tilde{r}^\xi\tilde{R}(\tilde{r}, z), \qquad \tilde{A}_\phi = \tilde{r}^2\tilde{A}, \quad (27)$$

where $\tilde{R}$ near $\tilde{r} = 0$ is a nonzero value. The particular redefinition of $\tilde{A}_\phi$ simplifies the numerical analysis. Our new equations of motion for these fields are:

$$\begin{aligned} &\partial_z^2\tilde{R} + \frac{f'}{f}\partial_z\tilde{R} + \frac{1}{f}\left(\partial_{\tilde{r}}^2\tilde{R} + \frac{2\xi + 1}{\tilde{r}}\partial_{\tilde{r}}\tilde{R} + \frac{\xi^2}{\tilde{r}^2}\tilde{R} - \frac{1}{\tilde{r}^2}\tilde{R}(\tilde{r}^2\tilde{A} - \xi)^2\right) + \frac{1}{f^2}\tilde{R}\tilde{A}_t^2 + \left(\frac{f'}{zf} - \frac{2}{z^2} + \frac{2}{z^2 f}\right)\tilde{R} = 0, \\ &\partial_z^2\tilde{A} + \frac{f'}{f}\partial_z\tilde{A} + \frac{1}{f}\left(\partial_{\tilde{r}}^2\tilde{A} + \frac{3}{\tilde{r}}\partial_{\tilde{r}}\tilde{A}\right) - \frac{\tilde{r}^{2\xi}}{f}\tilde{R}^2\left(\tilde{A} - \frac{\xi}{\tilde{r}^2}\right) = 0, \qquad \partial_z^2\tilde{A}_t + \frac{1}{f}\left(\partial_{\tilde{r}}^2\tilde{A}_t + \frac{1}{\tilde{r}}\partial_{\tilde{r}}\tilde{A}_t\right) - \frac{\tilde{r}^{2\xi}}{f}\tilde{R}^2\tilde{A}_t = 0. \end{aligned} \quad (28)$$

$$\begin{aligned} &\left[\partial_{\tilde{r}}^2\tilde{R} + \frac{2\xi + 1}{\tilde{r}}\partial_{\tilde{r}}\tilde{R} + \frac{\xi^2}{\tilde{r}^2}\tilde{R} - \frac{1}{\tilde{r}^2}\tilde{R}(\tilde{r}^2\tilde{A} - \xi)^2 - \tilde{R} = 3\partial_z\tilde{R}\right]_{z=1}, \qquad \left[\partial_z^2\tilde{R} = -\frac{1}{3}\tilde{R} - 2\partial_z\tilde{R} - \frac{1}{9}\tilde{R}(\partial_z\tilde{A}_t)^2\right]_{z=1}, \\ &\left[\partial_{\tilde{r}}^2\tilde{A} + \frac{3}{\tilde{r}}\partial_{\tilde{r}}\tilde{A} - \left(\tilde{A} - \frac{\xi}{\tilde{r}^2}\right)\tilde{r}^{2\xi}\tilde{R}^2 = 3\partial_z\tilde{A}_\phi\right]_{z=1}, \qquad [\partial_z^2\tilde{A} = -2\partial_z\tilde{A}]_{z=1}, \\ &\left[\partial_{\tilde{r}}^2\tilde{T} + \frac{1}{\tilde{r}}\partial_{\tilde{r}}\tilde{T} - \tilde{r}^{2\xi}\tilde{R}^2\tilde{T} = 6\partial_z\tilde{T}\right]_{z=1}, \quad [\partial_z^2\tilde{T} = -2\partial_z\tilde{T}]_{z=1}, \end{aligned} \quad (29)$$

where we have used that:

$$\lim_{z\to 1} A_t(\tilde{r}, z) = \lim_{z\to 1}(1 - z)\tilde{T}(\tilde{r}, z). \quad (30)$$

In particular, at the event horizon, we can expand the fields near $\tilde{r} = 0$ as:

$$\begin{aligned} \lim_{\tilde{r}\to 0}\tilde{R}(\tilde{r}, z) &= R_0(z)\left(1 + \frac{1}{2}a_2\tilde{r}^2 + O(\tilde{r}^3)\right), \\ \lim_{\tilde{r}\to 0}\tilde{A}(\tilde{r}, z) &= A_0(z)\left(1 + \frac{1}{2}b_2\tilde{r}^2 + O(\tilde{r}^3)\right), \\ \lim_{\tilde{r}\to 0}\tilde{T}(\tilde{r}, z) &= T_0(z)\left(1 + \frac{1}{2}c_2\tilde{r}^2 + O(\tilde{r}^3)\right). \end{aligned} \quad (31)$$

Substitution into the equation of motion at the horizon yields:

$$a_2 = \frac{R_0(1) + 3\partial_z R_0(1) - 2\xi A_0(1) R_0(1)}{2(\xi+1)R_0(1)},$$
$$b_2 = \begin{cases} \frac{A_0(1)R_0(1)^2 + 3\partial_z A_0(1)}{4A_0(1)}, & \xi = 0 \\ \frac{-\xi R_0(1)^2 + 3\partial_z A_0(1)}{4A_0(1)}, & \xi = 1 \\ \frac{3\partial_z A_0(1)}{4A_0(1)}, & \xi \geq 2 \end{cases}, \quad (32)$$
$$c_2 = \begin{cases} \frac{T_0(1)R_0(1)^2 + 6\partial_z T_0(1)}{2T_0(1)}, & \xi = 0 \\ \frac{6\partial_z T_0(1)}{2T_0(1)}, & \xi \geq 1 \end{cases}.$$

The solutions we study are characterized by the value of ξ and the $\tilde{r}$ asymptotic behavior of the field $\tilde{R}$. For any allowed value of ξ, the solution for $\tilde{R}$ can asymptote to zero or to a constant nonzero value.

We will be extracting nontrivial profiles for the fields at the boundary at $z = 0$ as follows:

$$\tilde{A}_t(\tilde{r}, z) = \mu(\tilde{r}) - \rho(\tilde{r}) z,$$
$$\tilde{A}_\phi(\tilde{r}, z) \equiv \tilde{r}^2 \tilde{A}(\tilde{r}, z) = a_\phi(\tilde{r}) + J_\phi(\tilde{r}) z, \quad (33)$$
$$\tilde{\rho}(\tilde{r}, z) \equiv z\tilde{R}(\tilde{r}, z) = \tilde{R}(\tilde{r}, 0) z + \partial_z \tilde{R}(\tilde{r}, 0) z^2,$$

where μ is related to the chemical potential, ρ is related to the charge density, J_ϕ is related to the azimuthal current, and a_ϕ is related to the magnetic field *via* $\tilde{B}_z = (\partial_{\tilde{r}} a_\phi)/\tilde{r}$. For the exact relationships, please consult Appendix A.

A. Droplet solutions

We consider the case of the case of $\xi = 0$, and use $\mathcal{O}_1$ as our order parameter. For this choice of ξ the solution that asymptotes to a constant value is simply the spatially-independent solution described earlier in Sec. III. In this section we consider solutions that asymptote to zero. To that end, we fix the following functions to:

$$\partial_z \tilde{R}(\tilde{r}, z = 1) = -\frac{1}{3}(1+\gamma)\tilde{R}(\tilde{r}, 1), \qquad \partial_z \tilde{A}(\tilde{r}, 1) = 0, \quad (34)$$

where γ is a positive number. With these choices, the equations of motion at the event horizon reduce to:

$$\left[\partial_{\tilde{r}}^2 \tilde{R} + \frac{1}{\tilde{r}}\partial_{\tilde{r}}\tilde{R} - \tilde{r}^2\tilde{A}^2\tilde{R} + \gamma\tilde{R}\right]_{z=1} = 0,$$
$$\left[\partial_z^2 \tilde{R} = \left(\frac{1}{3} + \frac{2}{3}\gamma\right)\tilde{R} - \frac{1}{9}\tilde{R}\tilde{T}^2\right]_{z=1},$$
$$\left[\partial_{\tilde{r}}^2 \tilde{A} + \frac{3}{\tilde{r}}\partial_{\tilde{r}}\tilde{A} - \tilde{R}^2\tilde{A}\right]_{z=1} = 0, \qquad [\partial_z^2 \tilde{A}]_{z=1} = 0, \quad (35)$$
$$\left[\partial_{\tilde{r}}^2 \tilde{T} + \frac{1}{\tilde{r}}\partial_{\tilde{r}}\tilde{T} - \tilde{R}^2\tilde{T} = 6\partial_z \tilde{T}\right]_{z=1},$$
$$\left[\partial_z^2 \tilde{T} = -2\partial_z \tilde{T}\right]_{z=1}.$$

The coefficients in Eq. (31) are given by:

$$a_2 = -\frac{\gamma}{2}, \qquad b_2 = \frac{R_0(1)^2}{4},$$
$$c_2 = \frac{T_0(1)R_0(1)^2 + 6\partial_z T_0(1)}{2T_0(1)}. \quad (36)$$

1. Numerical procedures

We begin by solving Eqs. (29), which are at the event horizon. For a given $R_0(1)$, we find that there is a specific value for $A_0(1)$ and $T_0(1)$ that gives regular solutions for the three functions $\tilde{R}(\tilde{r}, 1)$, $\tilde{A}(\tilde{r}, 1)$, $\tilde{T}(\tilde{r}, 1)$. The coupled ordinary differential equations are discretized using an explicit finite difference method, and we determine the values of $A_0(1)$ and $T_0(1)$ using a shooting method. By this we mean that we pick values for $A_0(1)$ and $T_0(1)$ at the origin and "shoot" towards $\tilde{r} \to \tilde{r}_{\max}$, where $\tilde{r}_{\max}$ is the largest radius out to which we will construct our solutions. Typically, this leads to a divergence in the functions, and therefore we iterate the procedure, fine–tuning our initial conditions such that a regular solution is found. This has now determined our initial conditions for the bulk problem.

The initial conditions at the event horizon having been determined, we solve the bulk equations of motion (28) and shoot towards the boundary at $z = 0$. The coupled partial differential equations are discretized using a finite difference method, and we adjust the mesh spacings Δz and Δr until we achieve stability for our code.

In order to satisfy the necessary boundary conditions at the AdS boundary, we try to minimize the *positive* area under the curve of $\partial_z \tilde{R}(\tilde{r}, 0)$. We accomplish this minimization by fine tuning our choice of $\partial_z T(\tilde{r}, 1)$ at the event horizon. This is achieved by expanding it in an appropriate basis of functions in $\tilde{r}$ and using a Monte-Carlo method to determine the coefficients (with the area playing the role of energy).

2. Sample solutions

To give a sense of how the solutions behave, we present multiple solutions for multiple values of γ and $\tilde{R}_0(1)$. The solutions are presented in Fig. 3. From Figs. 3(g) and 3(h) we see that for a given value of γ, for various initial condition values of the scalar field, we get the same asymptotic charge density. We learned from the spatially independent solution that the ratio of T/T_c is determined by the charge density, and therefore we learn that γ fixes the value of T/T_c. In fact, as $\gamma \to 0$, we have $T/T_c \to 1$ and as $\gamma \to \infty$, we have $T/T_c \to 0$. From Figs. 3(c) and 3(d), we see that the magnetic field asymptotes to a constant value, which indicates that the solutions "live" in a background magnetic field. As the magnitude of the scalar field increases, the value of this background magnetic field rises. Note also that how the magnetic field behaves in the core of the droplet varies considerably between low and high

temperatures. At low temperatures (Fig. 3(d)), the magnetic field is enhanced by the droplet, whereas as high temperatures (Fig. 3(c)), the droplet weakens the magnetic field in the "core." This variation in behavior suggests that these are perhaps not superconducting droplets as was thought [2,6].

We can try to study the minimum magnetic field needed to first form these droplet solutions. This would correspond to studying the problem in the limit where the magnitude of the scalar field is approaching zero, *i.e.* the perturbative or probe limit. In this limit, it is consistent to take $\tilde{A}$ to be a constant in both $\tilde{r}$ and $\tilde{z}$ and to take $\tilde{A}_t$ to only depend on z. The equation of motion for $\tilde{R}$ with $\tilde{A} = \gamma/2$ reduces to:

$$\left[\partial_{\tilde{r}}^2\tilde{R} + \frac{1}{\tilde{r}}\partial_{\tilde{r}}\tilde{R} - \frac{1}{4}\tilde{r}^2\gamma^2\tilde{R} + \gamma\tilde{R}\right]_{z=1} = 0. \tag{37}$$

This equation has (lowest energy) solution given by:

$$\tilde{R}(\tilde{r}, z = 1) = R_0(1)\exp\left(-\gamma\frac{\tilde{r}^2}{4}\right). \tag{38}$$

Next, we can solve for the z dependence by solving:

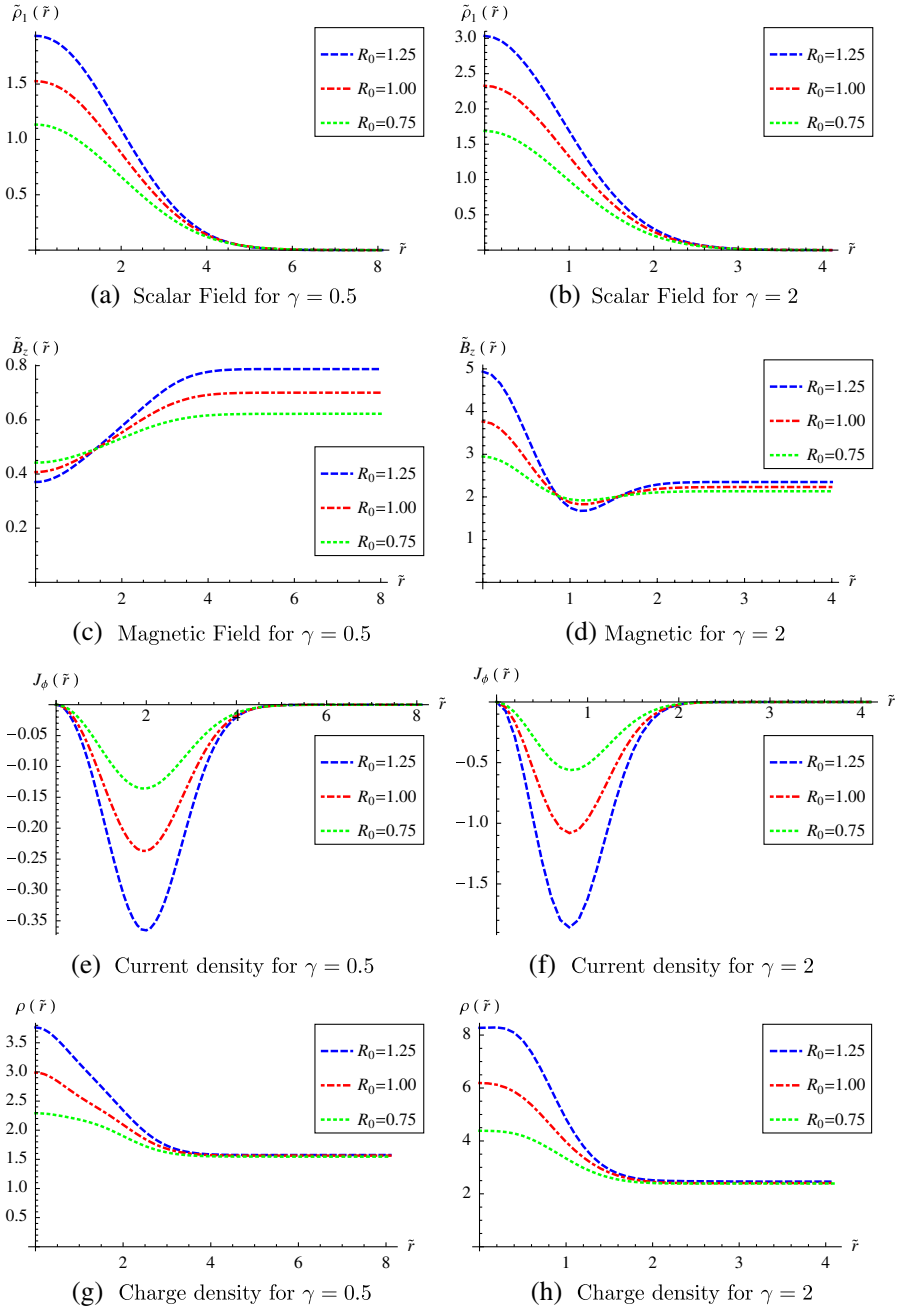

(a) Scalar Field for $\gamma = 0.5$ (b) Scalar Field for $\gamma = 2$

(c) Magnetic Field for $\gamma = 0.5$ (d) Magnetic for $\gamma = 2$

(e) Current density for $\gamma = 0.5$ (f) Current density for $\gamma = 2$

(g) Charge density for $\gamma = 0.5$ (h) Charge density for $\gamma = 2$

FIG. 3 (color online). Droplet solutions for $\gamma = 0.5$ on the left and $\gamma = 2$ on the right. They correspond to $T/T_c \approx 0.84$ and $T/T_c \approx 0.67$ respectively.

$$\partial_z^2\tilde{R} + \frac{f'}{f}\partial_z\tilde{R} - \frac{1}{f}\gamma\tilde{R} + \frac{1}{f^2}\tilde{R}\tilde{A}_t^2 + \left(\frac{f'}{zf} - \frac{2}{z^2} + \frac{2}{z^2 f}\right)\tilde{R} = 0,$$
$$\partial_z^2\tilde{A}_t = 0, \tag{39}$$

with the appropriate boundary conditions at the AdS boundary. This in turn fixes the value of the temperature of the solution. The value of the magnetic field found here corresponds to the critical magnetic field at which the droplet solutions first form. We draw the corresponding diagram in Fig. 4. The source of the divergence in the critical magnetic field as $T/T_c \to 0$ is clear. As the magnetic field and charge density grow in value, they begin to back–react on the geometry, and our decoupling breaks down. However, our results allow us to shed new light on the calculation done in Ref. [6]. There, the prototype solution in the droplet class was first uncovered in the probe limit. Now we see that the probe limit is the correct limit to study the onset of the droplets. So far in this section we have seen them in the decoupling $g \to \infty$ limit, and further taking the probe limit (*i.e.* the scalar is small and not backreacting on either Maxwell or Einstein) gives a limiting line at which they drop to zero height, ceasing to exist for lower B.

We can study this further (and extend to lower T/T_c) by working again in the probe limit, but at arbitrary g, as outlined in Sec. II C. Here, the background is now a charged black hole solution, our method of taking into account some of the backreaction of the gauge fields. In this limit the $\tilde{\rho}$ equation of motion is given by:

$$\partial_z^2\tilde{\rho} + \left(\frac{f'}{f} - \frac{2}{z}\right)\partial_z\tilde{\rho} + \frac{1}{f}\left(\partial_{\tilde{r}}^2\tilde{\rho} + \frac{1}{\tilde{r}}\partial_{\tilde{r}}\tilde{\rho} - g^2h^2\tilde{r}^2\tilde{\rho}\right) + \frac{(1-z)^2}{f^2}4g^2q^2\tilde{\rho} + \frac{2}{z^2 f}\tilde{\rho} = 0, \tag{40}$$

This equation has a separable solution that we write as:

$$\tilde{\rho} = zZ(z)R(\tilde{r}), \tag{41}$$

and we write their respective equations of motion as:

$$\partial_{\tilde{r}}^2 R + \frac{1}{\tilde{r}}\partial_{\tilde{r}}R - \frac{1}{4}\tilde{r}^2(4g^2h^2)R - 2ghR = 0, \tag{42}$$

$$\partial_z^2 Z + \frac{f'}{f}\partial_z Z - \frac{1}{f}2ghZ + \frac{(1-z)^2}{f^2}4g^2q^2Z + \left(\frac{2}{z^2 f} + \frac{f'}{fz} - \frac{2}{z^2}\right)Z = 0. \tag{43}$$

The solution for $R(\tilde{r})$ is given by:

$$R(\tilde{r}) = \exp(-gh\tilde{r}^2/2). \tag{44}$$

We can solve the equation for $Z(z)$ using the same arguments as before, and we get the solutions shown in Fig. 5. Our claim is that the perturbative scalar field on the dyonic black hole describes the entire phase transition line in the phase diagram, and the problem studied earlier is simply the $g \to \infty$ limit near $T/T_c \to 1$. To prove this, we do several nontrivial checks. First, we check that the dyonic theory can predict the critical temperature of the $g \to \infty$ theory. In order to do this, we make the identification:

$$2qg = \rho_{g\to\infty}, \tag{45}$$

by comparing the charge density of both theories. Next, we know that as the magnetic field approaches zero, the droplets appear at the critical temperature (or $T/T_c = 1$) for both theories. Given that we defined T_c in different ways for both theories, by setting them equal, we should be able to calculate the relationship between T_c and $\sqrt{\rho}$ that we saw in the $g \to \infty$ theory. In particular:

$$T_c/\alpha = \frac{1}{4\pi}(3 - q_c^2) = \sigma\sqrt{2gq_c}. \tag{46}$$

Therefore, we can solve for σ as $g \to \infty$. We present the results in Fig. 6. As one can see, in the limit of $g \to \infty$ we indeed recover the values 0.226 and 0.118, respectively, which were obtained earlier in the $g \to \infty$ probe case (see the caption of Fig. 2). We can also check whether the phase diagrams coincide. This is presented in Fig. 7. As we see, the dyonic black hole results very quickly approach our results for the $g \to \infty$ case for a range of T/T_c near one. We are now in a position to answer what happens when $T/T_c \to 0$ for the $g \to \infty$ limit. The zero temperature limit requires us to take:

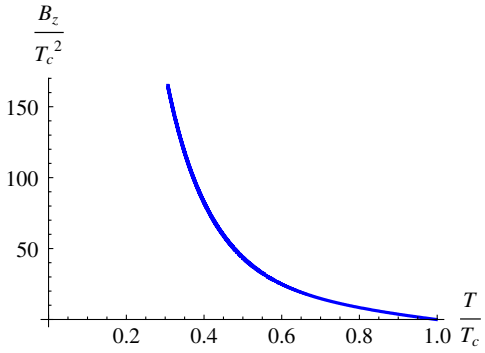

FIG. 4 (color online). The limiting droplet line in the $g \to \infty$ limit. Below this, droplets disappear.

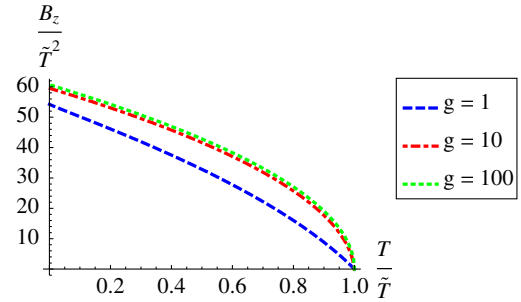

FIG. 5 (color online). Limiting droplet line for three values of g with $\tilde{T} = (3 - q_c^2)/4\pi$.

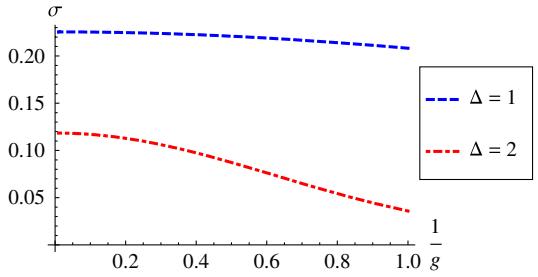

FIG. 6 (color online). Convergence to the $g \to \infty$ critical temperature. The curves asymptote to 0.225492 and 0.118412, respectively. See text for discussion.

$$q^2 + h^2 = 3. \tag{47}$$

As $g \to \infty$, we find that regularity of any solution at zero temperature requires us to take:

$$h \to \sqrt{3} - \frac{3}{2}\frac{1}{g}, \qquad q \to 3^{3/4}\frac{1}{\sqrt{g}}. \tag{48}$$

Therefore, the Gaussian profile in Eq. (44) vanishes in the limit of zero temperature and $g \to \infty$ (note that this does not happen at finite g). Therefore, the droplet no longer exists in that limit. Another way to see this is that in this limit, the dimensionless quantity gB_z/T_c^2 as used in Fig. 7 diverges.

B. Vortex solutions

We now consider solutions for the scalar that asymptote to a constant nonzero value. These are the vortex solutions.

1. Numerical procedures

The numerical procedure for the vortex is almost identical to that of the droplet (see Sec. IV A 1). We found it much more difficult to solve for the initial functions on the horizon using a shooting method, and so we inserted an initial guess function for an approximation to the scalar field $\tilde{R}(\tilde{r}, 1)$ at the event horizon, parametrized by two constants R_0 and R_1. We then use that function to solve for the field $\tilde{A}(\tilde{r}, 1)$, however it turns that for a given $A_0(1)$

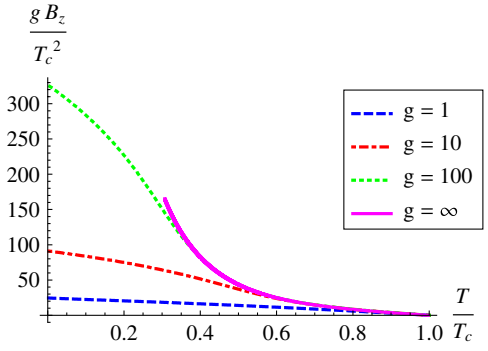

FIG. 7 (color online). The droplet limiting curves for a range of couplings, after rescaling to include the $g \to \infty$ case. $T_c = \alpha\sigma\sqrt{2qg}$.

and R_0, there is a specific R_1 that leads to a regular solution; we again use a shooting method to determine this constant. The constant $T_0(1)$ is determined in the same way. With both $\tilde{R}(\tilde{r}, 1)$ and $\tilde{A}(\tilde{r}, 1)$ determined, we have fully fixed $\partial_z\tilde{R}(\tilde{r}, 1)$. The bulk shooting problem is tackled as before. Note that the leading term in the expansion of $\partial_z\tilde{T}$ is the constant already determined in the spatially independent problem using Eqs. (21), since our vortices asymptote to that case.

2. Sample solutions

Here, we illustrate the case of $\xi = 1$ and $\xi = 2$ and again use $\mathcal{O}_1$ as our order parameter. We again consider the equations of motion given in Eqs. (28) and (29). For simplicity, we focus on the case of $\partial_z\tilde{A} = 0$. We note that as the solutions approach a constant value, they should asymptote to the spatially-independent solutions we have presented earlier. This in turn allows us to define the temperature at which a given solution exists. We present examples of such solutions in Figs. 8 and 9. In Fig. 8, we see that very far away from the origin, the scalar field has a constant vev, but as it approaches the core of the vortex, it decreases to zero value. The behavior at the origin is of course determined by the choice of ξ. The choice of ξ also influences how the gauge field $\tilde{A}_\phi$ behaves. In Figs. 9(g) and 9(h), we see that the value of $\tilde{A}_\phi$ asymptotes to the value of ξ. This is exactly the behavior required for the magnetic flux penetrating the vortex to be quantized with value $2\pi\xi$. We review this briefly in Appendix B. Indeed, ξ defines a nontrivial topological winding number: The scalar $\tilde{\rho}$ becomes constant at infinity, breaking the $U(1)$. Therefore the gauge symmetry of Eq. (23) cannot be used to unwind θ. Gauge symmetry is unbroken at infinity for the droplets, so ξ is not a winding number for them. The current density $J_\phi(\tilde{r})$ (Figs. 9(e) and 9(f)) is zero asymptotically and peaks in a ring around the core, supporting the magnetic field, as expected for a vortex.

In Fig. 9(b), we find that the charge density near the origin begins to oscillate as the density drifts downwards. It is difficult to say whether or not this is a physical attribute of the solutions or whether it is an artifact of our scheme to find the appropriate shooting functions that satisfy the $z = 0$ boundary condition. If they are physical, they may be caused by screening effects being strong in the core of the vortex. It is interesting to note that this behavior appears to be absent for the $\xi = 1$ vortex (see Fig. 9(a)), although we do see that there is a transition from the charge density increasing in the core to decreasing in the core as the temperature is lowered. Another curiosity for the $\xi = 1$ vortex is the behavior of the magnetic field near the origin (see Fig. 9(c)). Instead of flattening out as is the case for the $\xi = 2$ solutions, it dips slightly downwards. We expect this also to be a numerical artifact, since the $\xi = 1$ case is more numerically sensitive because of its sharper profile near $\tilde{r} = 0$.

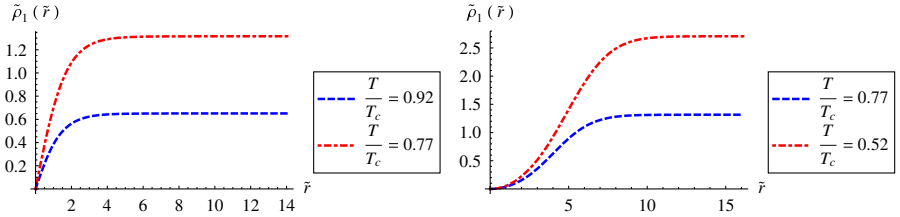

(a) Scalar Field (b) Scalar Field

FIG. 8 (color online). Vortex Solutions for $\xi = 1$ (lhs) and $\xi = 2$ (rhs).

V. CONCLUSION

We have constructed two broad families of localized solution to the equations of motion for Ref. [1]'s holographic model of a superconductor, and considered several of their key properties.

The vortices, with winding number ξ, contain $2\pi\xi$ units of magnetic flux, and are candidates to fill out the superconducting part of the phase diagram in the presence of an external magnetic field. This is because a lattice of them in the (r, ϕ) plane can trap flux lines of an applied external B–

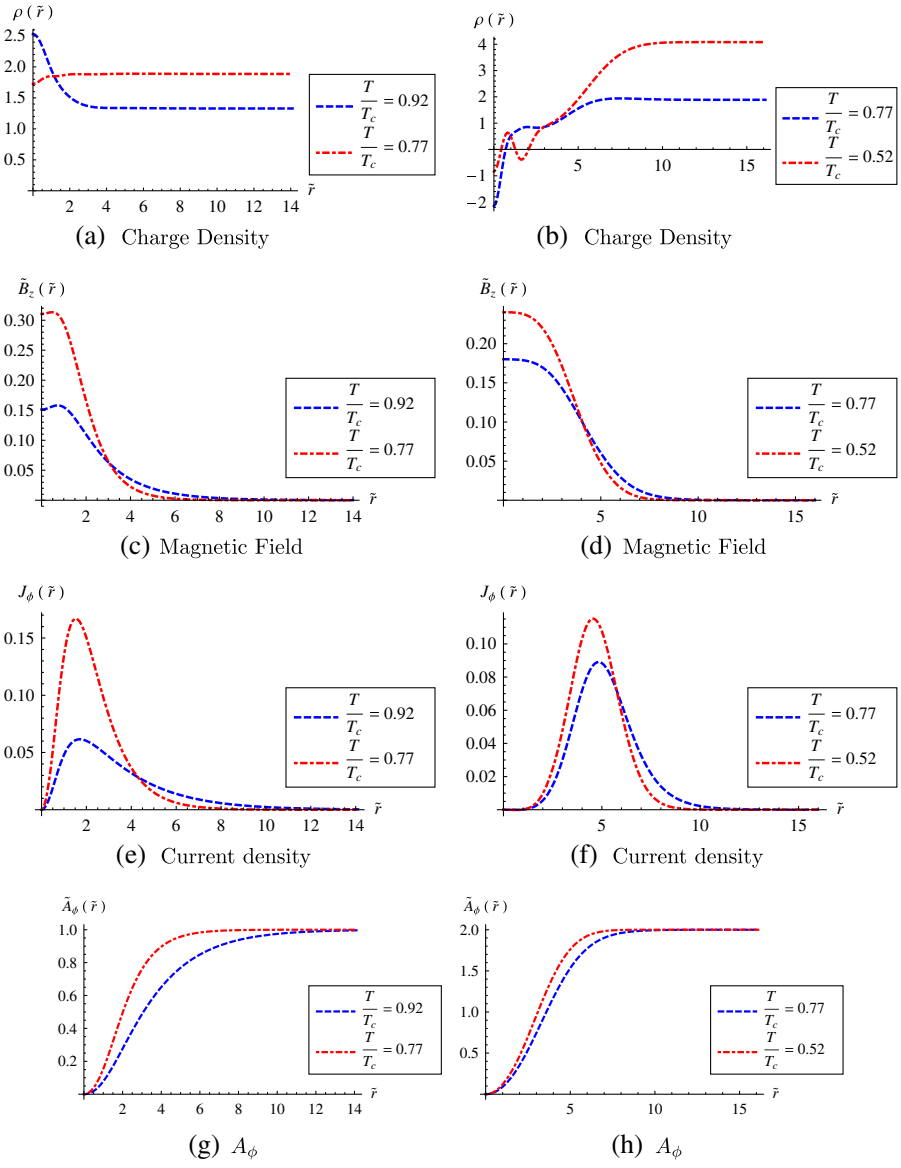

(a) Charge Density (b) Charge Density

(c) Magnetic Field (d) Magnetic Field

(e) Current density (f) Current density

(g) A_ϕ (h) A_ϕ

FIG. 9 (color online). Vortex Solutions for $\xi = 1$ (lhs) and $\xi = 2$ (rhs).

field into filaments as it passes through the two dimensional sample. Vortices presumably repel each other, and so such a lattice will cost energy. Therefore at some critical $B_c(T)$ the system will seek a lower energy phase, possibly returning to the normal phase. We have not constructed such a lattice, and further study to understand such a configuration is a very interesting avenue of research to pursue. Forming such a lattice is a method by which, at a given $T/T_c < 1$, the superconducting phase can be made to persist in some constant background B, even though the system cannot eject the magnetic field entirely *à la* the Meissner effect (there is a nice energetic argument in Ref. [2] as to why the Meissner effect is not possible in this two dimensional case). This vortex phase is of course the same method by which a standard type II superconductor can persist beyond the (lower) critical line at which the Meissner effect disappears, and we expect that it applies here. The study of multivortex solutions needed to establish this is left for further study.

Crucially, we have established that the droplets do not exist below a certain critical value of B, dropping to zero height on a family of lines that we were able to compute explicitly. For this and a variety of other stated reasons, and also considering the fact that they are of finite size and hence a lattice or gas of them would not give a connected superconducting path for charge transport, we believe that they do not represent a superconducting phase. (Hence, we disagree with the statements made about the phase diagram in Ref. [2]. The authors find the critical line, but state (similarly to our Ref. [6]) that the droplets exist *below* the line, and are superconducting. As they did not have the full droplet solutions, nor the vortex solutions, their analyses are not sufficient to make these determinations). They seem to represent a nonsuperconducting phase that is inhomogeneous. Whether or not the droplets are the favored solution for arbitrarily large B is an interesting question. There is the possibility that the system may prefer to return to the normal phase represented by a dyonic black hole with zero scalar. Which possibility is favored would be answered with an action computation to determine their relative free energies. However, such a calculation would require the fully (Einstein-Maxwell–Scalar) backreacted solutions. This is left for future work. We mention here that we also noticed the curious fact that the droplet solution at higher magnetic field (that we presented earlier) contains regions where the local value of the squared scalar mass is below the Breitenlohner-Freedman bound. This may point to an instability at large B that may be made more manifest by a complete study of the quasinormal modes of the droplets.

It would also be of interest to establish whether the critical line where the vortex phase would disappear coincides with the limiting line where the droplets' existence begins. We conjecture this to be likely on the grounds that we have found no other candidate solutions to fill an intermediate region. While this is the simplest possibility, further study is needed to establish it firmly.

ACKNOWLEDGMENTS

We would like to thank Arnab Kundu and Rob Myers for conversations. C. V. J. thanks the Aspen Center for Physics for a stimulating working atmosphere while this manuscript was prepared.

APPENDIX A: NORMALIZATIONS IN THE HOLOGRAPHIC DICTIONARY

We recall the AdS dictionary (working in Euclidean metric):

$$\left\langle \exp \int \phi_0 \mathcal{O} \right\rangle = \exp(-S_{\text{on-shell}}[\phi_0]) = \mathcal{Z}. \tag{A1}$$

Taking derivatives on both sides with respect to the boundary source ϕ_0 gives us our AdS dictionary:

$$\langle \mathcal{O}(x_1) \ldots \mathcal{O}(x_n) \rangle = (\beta \mathcal{V})^{-n} \lim_{\phi_0 \to 0} \mathcal{Z}^{-1} \frac{\delta}{\delta \phi_0(x_1)} \ldots \times \frac{\delta}{\delta \phi_0(x_n)} \mathcal{Z}. \tag{A2}$$

We define the free energy density of the dual theory to be given:

$$\mathcal{F} = \frac{1}{\beta \mathcal{V}} S_{\text{on shell}}, \tag{A3}$$

where β is the inverse temperature and $\mathcal{V}$ is the "spatial volume" of the dual theory. If we use the notation that we are working in AdS_{d+1}, then $\mathcal{V}$ has mass dimension $d-1$. For us, $d = 3$. In the Euclidean language, our action is given by:

$$S_{\text{bulk}} = \frac{1}{2\kappa_4^2} \int d^4x \sqrt{-G} \left\{ -R - \frac{6}{L^2} + L^2 \left(\frac{1}{4} F^2 + |\partial \Psi - igA\Psi|^2 + \mathcal{V}(|\Psi|) \right) \right\}, \tag{A4}$$

where we emphasize that although the metric is now purely positive, we are still using A_t and now a Wick rotated version of it. In the dual theory, the charge density is given by:

$$\rho(x) = -\frac{\delta \mathcal{F}}{\delta \mu(x)}, \tag{A5}$$

where μ is the chemical potential and x represents the space-time coordinates in the dual field theory. Using the AdS/CFT dictionary, we can write:

$$\frac{\delta \mathcal{F}}{\delta \mu(x)} = \frac{1}{\beta \mathcal{V}} \frac{\delta S_{\text{on-shell}}}{\delta A_t(x, 0)}. \tag{A6}$$

Using the action given in Eq. (A4), we find:

$$\frac{g}{\beta\mathcal{V}}\frac{\delta S_{\text{on-shell}}}{\delta A_t(x,0)} = \frac{L^2}{2\kappa_4^2}\frac{1}{g}\alpha\partial_z A_t(x,0) = \frac{L^2}{2\kappa_4^2}\frac{1}{g}\alpha^2\partial_z\tilde{A}_t(x,0), \tag{A7}$$

where we have used that:

$$\frac{\delta A_t(x')}{\delta A_t(x)} = \beta\mathcal{V}\delta^{(d+1)}(x'-x). \tag{A8}$$

and we have dropped the contribution coming from the event horizon. Therefore, the end result is given by:

$$\rho(x) = -\frac{L^2}{2\kappa_4^2}\frac{1}{g}\alpha^2\partial_z\tilde{A}_t(x,0). \tag{A9}$$

A similar procedure allows us to calculate the vev of the azimuthal current as well:

$$J^\phi(x) = -g\beta\mathcal{V}\frac{\delta S_{\text{on-shell}}}{\delta A_\phi(x)} = \frac{L^2}{2\kappa_4^2}\frac{1}{g}\frac{\alpha^3}{\tilde{r}^2}\partial_z\tilde{A}_\phi. \tag{A10}$$

Note that here we are using the vector field that has been rescaled by g, hence why the factor of g appears at the beginning of our definition. Next, we can calculate the form of the vevs of the $\Delta = 1$ and $\Delta = 2$ operators. To proceed, we take the $\Delta = 1$ operator to be the source of the $\Delta = 2$ operator [8]. Therefore, we write:

$$\langle\mathcal{O}_2(x)\rangle = -\frac{\delta\mathcal{F}}{\delta\langle\mathcal{O}_1(x)\rangle} \propto -\frac{\delta\mathcal{F}}{\delta\rho_1(x)}, \tag{A11}$$

where we are using the notation that:

$$\rho(x, z\to 0) = z\rho_1(x) + z^2\rho_2(x). \tag{A12}$$

To proceed, we calculate the variation of the bulk action (keeping only divergent and finite terms):

$$\delta S_{\text{bulk}} = -\lim_{z\to 0}\frac{L^2}{2\kappa_4^2}\frac{1}{g^2}\int d^3x L^2\alpha^3\Big(\frac{1}{z}\rho_1(x)\delta\rho_1(x) + 2\rho_2(x)\delta\rho_1(x) + \rho_1(x)\delta\rho_2(x)\Big). \tag{A13}$$

The first term in parentheses is divergent, but it is removed by an appropriate counterterm:

$$S_{\text{CT}} = -\frac{L^2}{2\kappa_4^2}\frac{1}{g^2}\lim_{z\to 0}\frac{\sqrt{-\gamma}}{L}\int d^3x\frac{1}{2}\rho(x,z)^2, \tag{A14}$$

which leaves us with:

$$\delta S_{\text{bulk}} + \delta S_{\text{CT}} = -\frac{L^2}{2\kappa_4^2}\frac{1}{g^2}\int d^3x L^2\alpha^3\rho_2(x)\delta\rho_1(x). \tag{A15}$$

Therefore, we find:

$$-\frac{1}{\alpha L}\frac{\delta\mathcal{F}}{\delta\rho_1(x)} = \frac{L^2}{2\kappa_4^2}\frac{1}{g^2}L\alpha^2\rho_2(x) = \frac{L^2}{2\kappa_4^2}\frac{1}{g^2}\alpha^2\tilde{\rho}_2(x). \tag{A16}$$

To calculate the vev of the $\Delta = 1$ operator, we need to perform a Legendre transform on $\mathcal{F}$ [8]:

$$\mathcal{G} = -\mathcal{F} - \frac{1}{\beta\mathcal{V}}\frac{L^2}{2\kappa_4^2}\frac{L^2\alpha^3}{g^2}\int d^3x\rho_1(x)\rho_2(x), \tag{A17}$$

and we now have:

$$-\frac{1}{L\alpha^2}\frac{\delta\mathcal{G}}{\delta\rho_2(x)} = \frac{L^2}{2\kappa_4^2}\frac{1}{g^2}L\alpha\rho_1(x) = \frac{L^2}{2\kappa_4^2}\frac{1}{g^2}\alpha\tilde{\rho}_1(x). \tag{A18}$$

Therefore, in order to satisfy the conditions:

$$\langle\mathcal{O}_2(x)\rangle = -\frac{\delta\mathcal{F}}{\delta\langle\mathcal{O}_1(x)\rangle}, \qquad \langle\mathcal{O}_1(x)\rangle = -\frac{\delta\mathcal{G}}{\delta\langle\mathcal{O}_2(x)\rangle}, \tag{A19}$$

we choose:

$$\langle\mathcal{O}_1(x)\rangle = \frac{L}{\sqrt{2}g\kappa_4}L\alpha\rho_1(x) = \frac{L}{\sqrt{2}g\kappa_4}\alpha\tilde{\rho}_1(x), \tag{A20}$$

$$\langle\mathcal{O}_2(x)\rangle = \frac{L}{\sqrt{2}g\kappa_4}L\alpha^2\rho_2(x) = \frac{L}{\sqrt{2}g\kappa_4}\alpha^2\tilde{\rho}_2(x). \tag{A21}$$

APPENDIX B: FLUX QUANTIZATION

Let us review the flux quantization condition. Deep in the superconductor, away from the vortex, our results indicate that we have $\tilde{A}_\phi = \xi$. This can be written as:

$$\frac{1}{r}A_\phi = \frac{1}{r}\partial_\phi\theta. \tag{B1}$$

It is useful at this point to realize that A_ϕ/r transforms exactly as the vector $\vec{A}$. Therefore, it is convenient to write Eq. (B1) as:

$$\vec{\nabla}\theta = \vec{A}. \tag{B2}$$

Consider drawing a circle around the vortex, deep in the superconductor. We can choose to integrate Eq. (B1) along the circle:

$$\oint\vec{\nabla}\theta\cdot d\vec{\ell} = \oint\vec{A}\cdot d\vec{\ell}. \tag{B3}$$

where A is the corresponding 1-form. The left-hand side (lhs) gives $2\pi\xi$, and using Stokes' theorem on the right-hand side (rhs), we have:

$$2\pi\xi = \int(\vec{\nabla}\times\vec{A})_z da = \int da\Big(\frac{1}{r}\partial_r A_\phi\Big). \tag{B4}$$

Note that the quantity in brackets on the right is exactly the magnetic field, so we find that the flux of a single vortex is quantized to $2\pi\xi$.

[1] S. A. Hartnoll, C. P. Herzog, and G. T. Horowitz, Phys. Rev. Lett. **101**, 031601 (2008).
[2] S. A. Hartnoll, C. P. Herzog, and G. T. Horowitz, J. High Energy Phys. 12 (2008) 015.
[3] S. S. Gubser, Phys. Rev. D **78**, 065034 (2008).
[4] M. Ammon, J. Erdmenger, M. Kaminski, and P. Kerner, Phys. Lett. B **680**, 516 (2009).
[5] M. Ammon, J. Erdmenger, M. Kaminski, and P. Kerner, J. High Energy Phys. 10 (2009) 067.
[6] T. Albash and C. V. Johnson, J. High Energy Phys. 09 (2008) 121.
[7] P. Breitenlohner and D. Z. Freedman, Phys. Lett. B **115**, 197 (1982).
[8] I. R. Klebanov and E. Witten, Nucl. Phys. **B556**, 89 (1999).
[9] A. Chamblin, R. Emparan, C. V. Johnson, and R. C. Myers, Phys. Rev. D **60**, 064018 (1999).
[10] G. W. Gibbons and S. W. Hawking, Commun. Math. Phys. **66**, 291 (1979).
[11] L. J. Romans, Nucl. Phys. **B383**, 395 (1992).